In Vivo X-Ray Imaging Reveals Improved Airway Surface Hydration after a Therapy Designed for Cystic Fibrosis

To the Editor:

Sufficient airway surface liquid (ASL) depth is critical to ensure that the mucociliary transport system can effectively clear inhaled pathogens from the lungs. In those with cystic fibrosis (CF), the CF transmembrane conductance regulator gene defect decreases airway surface hydration (1, 2), compromising lung defense mechanisms, resulting in progressive lung infection and early death (3). An effective CF respiratory therapy should increase the ASL depth, restoring clearance mechanisms, but it is difficult to measure this depth *in vivo*. Current clinical health measures used for CF drug development studies include lung function testing and structural lung imaging (i.e., computed tomography), both indirect and delayed measures of airway hydration. Although the ASL depth has been measured by confocal microscopy in epithelial cultures (1, 4) and histologically in fragments of trachea (5), these technologies are not feasible *in vivo*.

We have realized a technique called single-grid–based phase–contrast X-ray imaging (SGB-PCXI) (Figure 1A) (6–9), which is capable of non-invasive ASL imaging, and we previously demonstrated its ability to measure the ASL rehydrating effects of aerosolized hypertonic saline (HS) in the excised trachea of a mouse (10). In this letter, we report the first *in vivo* measures of ASL using this technique.

PCXI methods capture information on how the sample refracts the X-ray wavefield to provide exquisite soft tissue images. This differs from conventional X-ray imaging, where absorption of the X-ray wavefield provides very little soft tissue contrast (11). ASL measurements were not feasible with previous PCXI methods, which lacked either the speed to capture these high-magnification images without motion blur, or the sensitivity to differentiate ASL from surrounding tissue. Our SGB-PCXI method provides the necessary speed and sensitivity by illuminating the airways with a grid pattern. At the image detector, the grid will appear distorted according to the refractive properties of the airway tissue, in the same way the tile pattern on the bottom of a swimming pool will appear distorted according to the refractive properties of the water (10). By analyzing these distortions, we can quickly and sensitively produce an image of the ASL (6–8).

Using SGB-PCXI, we measured the effects of a two-agent rehydrating treatment—an aerosol containing a long-acting epithelial sodium channel blocker (P308; Parion Sciences, Durham, NC), at a concentration of 1 mM in 7% HS—on ASL depth in live, anesthetized mice. C57Bl/6 mice (n = 14) were prepared for ventilation and imaging, as previously detailed (12), and placed in a supine position so that the ventral surface could be imaged to avoid multiple overlaid tracheal edges and ensure that any bulk fluid formed during aerosol delivery did not pool in the field of view. Treatments were delivered using an Aeroneb Pro nebulizer (Aerogen, Galway, Ireland), designed to produce 3.5-μm volume median diameter aerosol, integrated in the ventilator system, for a period of 90 seconds, 50% duty cycle. For each mouse, images of the ventral tracheal surface were captured at 3-minute intervals, before and for 15 minutes after delivery of the control (isotonic saline) treatment; after a break of 5 minutes, the 15-minute imaging sequence was repeated in the same mouse then being delivered the HS-P308 treatment (Figure 1D).

Before any image analysis was performed, six mice were rejected from the study (leaving n = 8). One mouse shifted position such that the airway moved out of the field of view; for two mice, the custom-built nebulizer control system malfunctioned; and in three mice, the intubation was placed too deeply into the airway for tracheal aerosol delivery (with the position observed immediately when X-ray imaging began). This failure rate illustrates the initial technical difficulty involved with these complex experiments, but sufficient sample size remained. We anticipate that these problems will decrease with experience, as in our previous imaging development work.

Measurements were made (observer blinded to treatment) by manually tracing the tissue–cartilage, tissue–ASL, and ASL–airway interfaces. Manual traces showed an acceptably high intraclass correlation of 0.992 between five different scorers in our previous study (10). The distance between marked interface lines was measured computationally, taking the average distance over the length of airway traced in that image. Measures taken at all time points were then analyzed by repeated-measures ANOVA (Prism 5; GraphPad, San Diego, CA).

Although the presence of overlying tissue and skin *in vivo* reduces the visibility of the subtle ASL–tissue interface compared with our previous *ex vivo* studies (10), ASL depth measurements were still possible, as seen by the *left bracket* in Figure 1B. The HS-P308 sequences showed lumen movement and increased ASL depth after treatment delivery (Figure 1C). The control (isotonic saline) sequences showed very little movement throughout, and this low, stationary ASL made it difficult to reliably identify the ASL–tissue interface, particularly given the obscuring influence of overlying skin/tissue. Therefore, to quantify biological changes in response to isotonic saline versus HS-P308, we measured the distance between the outer edge of a reference cartilage ring and the ASL–airway lumen interface, as indicated by the *bracket* in the *right* of Figure 1B.

A statistically significant increase in the position of the ASL surface (relative to the cartilage) was observed in the airways treated with HS-P308 compared with the earlier isotonic saline treatment for all time points after and including 6 minutes after aerosol delivery, as seen in Figure 1D. In the direct measures of ASL depth (Figure 1C) there was a significant increase in depth compared with baseline at 9 and 12 minutes after delivery of

Supported by Parion Sciences (P308; Durham, NC). The Japan Synchrotron Radiation Research Institute provided use of beamline BL20XU at the SPring-8 Synchrotron (experiment nos. 2012A1661 and 2013B1764). Travel funding was provided by the International Synchrotron Access Program, managed by the Australian Synchrotron and funded by the Australian government, and studies were supported by the Australian National Health and Medical Research Council (NHMRC) and the Cure4CF Foundation. K.S.M. was supported by an Australian Research Council Discovery Early Career Researcher Award (DE120102571), M.D. by an M. S. McLeod Fellowship, A.F. by an NHMRC Career Development Fellowship, and N.F. by an M. S. McLeod Ph.D. Scholarship.

Author Contributions: K.S.M., M.D., K.K.W.S., and D.W.P. designed and performed the experiments. A.F. and N.F. also performed the experiments and N.Y., Y.S., A.T., and K.U. provided expert assistance at the SPring-8 synchrotron beamline. K.S.M. developed the methodology, analyzed the data, and wrote the paper. D.W.P., M.D., R.C.B., and K.K.W.S. contributed to the writing and editing of the manuscript.

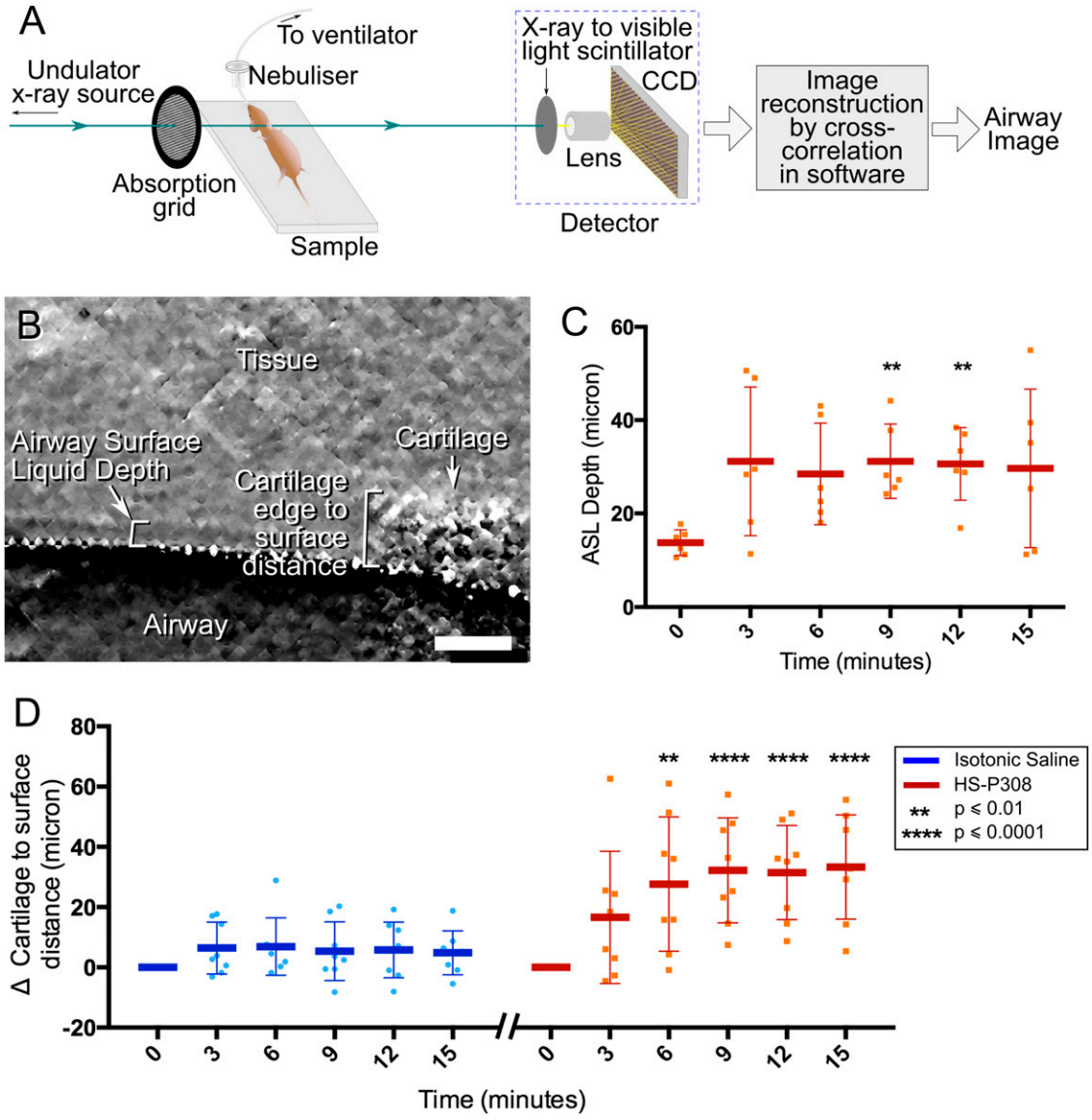

Figure 1. (*A*) Experimental setup using 25-keV X-rays at beamline BL20XU at the SPring-8 synchrotron in Japan, using the setup described in Reference 10, with a gold absorption grid of 25.4-μm period (Gilder grids, G1000HS-G3), and distances of 0.1 m grid-to-sample and 1 m sample-to-detector. The lens-coupled charge-coupled device detector captures a 721 × 497-μm field of view with 0.18-μm pixels using a 100-ms exposure. Airway images are reconstructed using a correlation-based analysis detailed in References 6–8. (*B*) Single-grid–based phase–contrast X-ray imaging (SGB-PCXI) differential contrast image of the *in vivo* trachea surface. *Scale bar* = 100 μm. (*C*) Airway surface liquid (ASL) depth measurements, where each data point represents a measurement, and the *darker bars* indicate the mean (±SD) of measurements at that time point. Hypertonic saline (HS)–P308 was delivered after the t = 0 time point, analyzed by one-way repeated-measures (RM)-ANOVA to detect differences compared to baseline (t = 0). Statistical significance was set at a *P* value of 0.05 and a power of 0.8 for all analyses. (*D*) Changes in the cartilage-to-surface distance over time, analyzed by two-way RM-ANOVA with Bonferroni multiple comparisons to detect significant differences between treatments at matching time points. In the 5-minute break between sequences, researchers entered the imaging hutch to change the treatment solution.

HS-P308. Although some mice showed a large increase within 3 minutes of treatment delivery, others had a more delayed effect, resulting in a large spread of values at 3 minutes. A similarly large spread of values was seen at 15 minutes, when the treatment effect may have waned for some of the mice, increasing the variability of the dataset at that final time point.

The relative increase in the ASL depth was of similar magnitude to that seen in our *ex vivo* study (10), with the average depth increasing by a maximum of 10–15 μm. This effect is consistent in magnitude and duration with tissue culture studies (13). It is interesting to note that the increase in the cartilage-to-airway measure (Figure 1D) was greater than the increase in ASL depth measure (Figure 1C, subtracting baseline), peaking at around 30 μm compared with 10 μm. This finding suggests that there may be additional liquid drawn from surrounding tissue into the submucosal compartment, causing that region to swell and raise the surface of the liquid further from the cartilage. In contrast, our *ex vivo* studies observed a decrease in airway tissue volume from 3 minutes

after treatment, when there was no surrounding tissue present (10). This difference illustrates the importance of conducting studies *in vivo* when assessing a physiological response to treatment. We also noted that the treatment effect lasted longer *in vivo* with HS-P308 treatment compared with *ex vivo* with HS treatment. Because both the treatment agent and the nature of the measurements (*in/ex vivo*) were different between this and previous studies, we cannot determine which factor produced this extended effect.

We believe that these are the first reported noninvasive *in vivo* measurements of changes in ASL volume (depth) in response to an airway-rehydrating treatment. Our transition from *ex vivo* to *in vivo* imaging is significant, enabling biologically relevant results, longitudinal studies, and treatment delivery technique studies. The research and clinical utilities of a rapid, noninvasive ASL depth measurement technique are significant. Although clinical implementation presents some challenges, continuing developments in image detectors and compact X-ray sources suitable for PCXI mean that this is still a possibility, although some compromises in image quality may be necessary to reduce radiation dose. In addition, these kinds of technical developments will certainly improve the accessibility, speed, and spatial resolution of our technique for research (note the use of light at X-ray wavelengths means that our images are several orders of magnitude from the fundamental spatial resolution limits). Direct observations of *in vivo* changes in the ASL depth immediately after application of known or potential therapies can lead to a better understanding of how CF transmembrane conductance regulator gene, protein, and channel activity alterations influence fundamental airway surface ion–water balance processes. Furthermore, rapid and accurate *in vivo* physiological outcome assessments of drugs emerging from the CF pharmaceutical development pipeline can be made at the site of action, and reveal biophysical mechanisms that precede more global measurements of airway function (e.g., FEV_1). Studies can also examine a range of disease models, and the noninvasive nature of this new measure means that repeat measures can be captured on the same animals across a range of time scales (14). ■

Author disclosures are available with the text of this letter at www.atsjournals.org.

Acknowledgment: The authors thank Parion Sciences for providing the P308 treatment. They also thank Charlene Chua, who provided expert technical assistance during the experimental procedures.

Kaye S. Morgan, Ph.D.
Monash University
Clayton, Victoria, Australia

Martin Donnelley, Ph.D.
Nigel Farrow
Women's and Children's Hospital
North Adelaide, South Australia, Australia
and
Robinson Institute, University of Adelaide
Adelaide, South Australia, Australia

Andreas Fouras, Ph.D.
Monash University
Clayton, Victoria, Australia

Naoto Yagi, Ph.D.
Yoshio Suzuki, Ph.D.
Akihisa Takeuchi, Ph.D.
Kentaro Uesugi, Ph.D.
SPring-8/Japan Synchrotron Radiation Research Institute
Kouto, Hyogo, Japan

Richard C. Boucher, M.D.
University of North Carolina
Chapel Hill, North Carolina

Karen K. W. Siu, Ph.D.*
Monash University
Clayton, Victoria, Australia

David W. Parsons, Ph.D.*
Women's and Children's Hospital
North Adelaide, South Australia, Australia
and
Robinson Institute, University of Adelaide
Adelaide, South Australia, Australia

*K.K.W.S. and D.W.P. contributed equally as senior authors.

References

1. Matsui H, Grubb BR, Tarran R, Randell SH, Gatzy JT, Davis CW, Boucher RC. Evidence for periciliary liquid layer depletion, not abnormal ion composition, in the pathogenesis of cystic fibrosis airways disease. *Cell* 1998;95:1005–1015.
2. Boucher RC. Evidence for airway surface dehydration as the initiating event in CF airway disease. *J Intern Med* 2007;261:5–16.
3. Daviskas E, Anderson SD. Hyperosmolar agents and clearance of mucus in the diseased airway. *J Aerosol Med* 2006;19:100–109.
4. Donaldson SH, Bennett WD, Zeman KL, Knowles MR, Tarran R, Boucher RC. Mucus clearance and lung function in cystic fibrosis with hypertonic saline. *N Engl J Med* 2006;354:241–250.
5. Song Y, Namkung W, Nielson DW, Lee JW, Finkbeiner WE, Verkman AS. Airway surface liquid depth measured in *ex vivo* fragments of pig and human trachea: dependence on Na^+ and Cl^- channel function. *Am J Physiol Lung Cell Mol Physiol* 2009;297:L1131–L1140.
6. Morgan KS, Paganin DM, Siu KKW. Quantitative X-ray phase–contrast imaging using a single grating of comparable pitch to sample feature size. *Opt Lett* 2011;36:55–57.
7. Morgan KS, Paganin DM, Siu KKW. Quantitative single-exposure X-ray phase contrast imaging using a single attenuation grid. *Opt Express* 2011;19:19781–19789.
8. Morgan KS, Modregger P, Irvine SC, Rutishauser S, Guzenko VA, Stampanoni M, David C. A sensitive X-ray phase contrast technique for rapid imaging using a single phase grid analyzer. *Opt Lett* 2013;38: 4605–4608.
9. Morgan KS, Paganin DM, Parsons DW, Donnelley M, Yagi N, Uesugi K, Suzuki Y, Takeuchi A, Siu KKW. Single grating X-ray imaging for dynamic biological systems. *AIP Conf Proc* 2012;1466:124–129.
10. Morgan KS, Donnelley M, Paganin DM, Fouras A, Yagi N, Suzuki Y, Takeuchi A, Uesugi K, Boucher RC, Parsons DW, *et al*. Measuring airway surface liquid depth in *ex vivo* mouse airways by X-ray imaging for the assessment of cystic fibrosis airway therapies. *PLoS One* 2013;8:e55822.
11. Bravin A, Coan P, Suortti P. X-ray phase–contrast imaging: from pre-clinical applications towards clinics. *Phys Med Biol* 2013;58:R1–R35.
12. Donnelley M, Parsons D, Morgan K, Siu K. Animals in synchrotrons: overcoming challenges for high-resolution, live, small-animal imaging. *AIP Conf Proc* 2010;1266:30–34.
13. Tarran R, Grubb BR, Parsons D, Picher M, Hirsh AJ, Davis CW, Boucher RC. The CF salt controversy: *in vivo* observations and therapeutic approaches. *Mol Cell* 2001;8:149–158.
14. Donnelley M, Morgan KS, Siu KKW, Fouras A, Farrow NR, Carnibella RP, Parsons DW. Tracking extended mucociliary transport activity of individual deposited particles: longitudinal synchrotron imaging in live mice. *J Synchrotron Radiat* 2014;21:768–773.